Mathematical Ship Modeling for Control Applications

by

Tristan Pérez† and Mogens Blanke‡

Technical Report

†Dept. of Electrical and Computer Engineering
The University *of* Newcastle, NSW, 2308, Australia

‡Section of Automation at Ørsted.DTU
Technical University of Denmark, Building 326
DK-2800 Kgs. Lyngby, Denmark

Abstract

In this report, we review the models for describing the motion of a ship in four degrees of freedom suitable for control applications. We present the hydrodynamic models of two ships: a container and a multi-role naval vessel. The models are based on experimental results in the four degrees of freedom roll planar motion mechanism (RPMM) facility at the Danish Maritime Institute, and have also been validated via extensive full scale trials. Based on the RPMM hydrodynamic models, we also present non-linear and linearized state space models suitable for simulation and control applications. Finally, we evaluate the quality of the linearized models with respect to their nonlinear counterparts and analyze sensitivity to parameter variations.

1 Introduction

Essential to any control design is the knowledge of the dynamic characteristics of the plant or physical system to be controlled. Experimental work in the area of maneuvering and control of ships suggests that it is difficult to predict the maneuvering characteristics of a ship from model test due to the lack of precise knowledge of the steering and roll interaction (Blanke and Jensen, 1997). Thus, a great research effort has been made to analyze the dynamic involved in this interaction. The knowledge of the dynamics associated with roll, yaw and sway is not only useful to improve maneuvering models but also, for example, essential to the the application of rudder roll damping since the performance of this technique relies to a great extent on dynamic couplings between roll, yaw, and sway.

Although, the four degrees of freedom models for describing the motion of ships are well known, see for example (Abkowitz, 1975) and (Chislett and Støm-Tejsen, 1965), the magnitudes of the couplings to roll have been less well established (Blanke *et al.*, 1989). Therefore, models describing the interaction between roll sway and yaw have only been scarcely studied. For example, results published by Son and Nomoto (1982) present a model obtained by combining planar motion mechanism (PMM) test data for lateral motion, using different values of static heel for the model under test, with independent roll motion tests. Kälström and Otterson (1983) obtained a model by combining a lateral PMM model with theoretical estimates of roll coefficients, using free sailing model tests to calibrate the roll parameters. In this report, we present models based on experimental results in the unique 4-DOF roll planar motion mechanism (RPMM) facility at the Danish Maritime Institute that allow model testing with full dynamic interaction between motions in roll, sway, yaw and surge. This models capture the tight steering and roll interaction experienced in the vessels making them a valuable tool for the design of control strategies. The models have also been subject to validation via full-scale sea trials (Blanke *et al.*, 1989), (Blanke and Jensen, 1997).

Although parts of these models have been previously presented in different publications (Blanke, 1981) (Blanke

and Christensen, 1993) (Blanke and Jensen, 1997), it is still difficult to find in the literature fully-parameterized models. Therefore, the main contribution of this report is to revise the previously published material and to provide a self-contained document with detailed and fully-parameterized non-linear and linear state space models that can be utilized as a basis for analysis and design of ship motion control strategies. In addition, we present some simulation results to access the quality of the obtained linearized models, and perform a numerical analysis of the sensitivity of the models to parameter variations.

The rest of the report is organized as follows. In section 2, the ship dynamics in four degrees of freedom are reviewed. In section 3, the hydrodynamic models for forces and moments on the hull based on the RPMM are given. In section 4, the essentials of propulsion effects modelling and resistance are reviewed. In section 5, models describing the rudder produced forces and moments are given based on both physical modelling and RPMM. The results are then generalized to any movable fin on the hull. In section, 6, a simplified model for the steering machinery commonly utilized in control applications is reviewed. In section 7, the non-linear and linearized state space models for a container ship and a multi-role naval vessel are given. In section 8, some simulation results are presented to access the performance linear models obtained from the RPMM non-linear models, and numerical analysis of the sensitivity of the models to parameter variations is given. Finally, In section 9, we summarize and discuss the presented material.

2 Ship Dynamics: Newtonian approach

In this section, we review the mathematical models for describing the ship dynamics in four degrees of freedom.

The motion of a ship in six degrees of freedom is considered as a traslation motion (position) in three

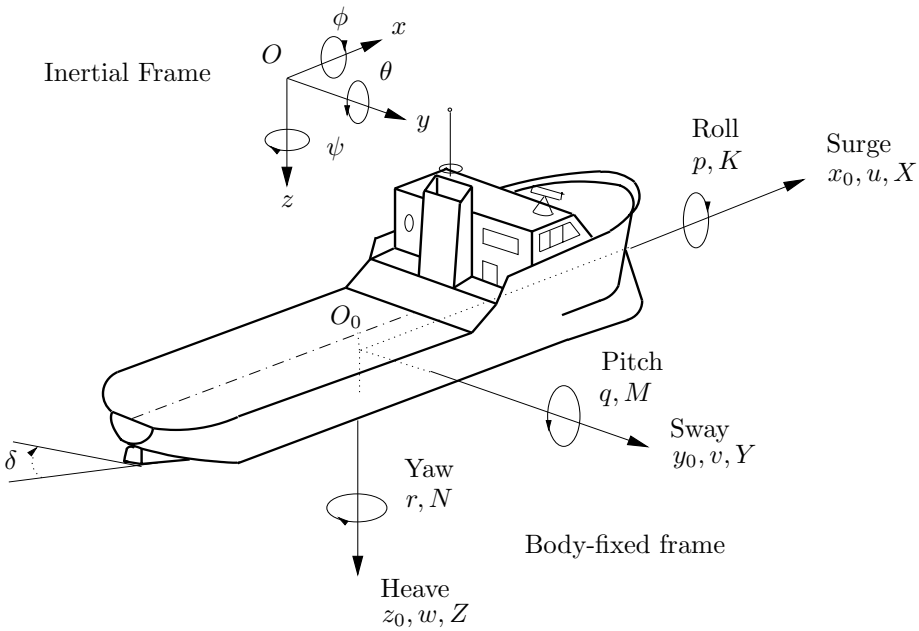

Figure 1: Standard notation and sign conventions for ship motion description (SNAME, 1950).

directions: surge, sway, and heave; and as a rotation motion (orientation) about three axis: roll, pitch and yaw. To determine the equations of motion, two reference frames are considered: the inertial or fixed to earth frame O that may be taken to coincide with the ship-fixed coordinates in some initial condition and the body-fixed frame O_0— see figure 1. For surface ships, the most commonly adopted position for the body-fixed frame is such it gives hull symmetry about the x_0z_0-plane and approximate symmetry about the y_0z_0-plane, while the origin of the z_0 axis is defined by the calm water surface (Price and Bishop, 1974).

The magnitudes describing the position and orientation of the ship are usually expressed in the inertial frame and the coordinates are noted: $[x \quad y \quad z]^{\mathrm{T}}$ and $[\phi \quad \theta \quad \psi]^{\mathrm{T}}$ respectively, whilst the forces $[X \quad Y \quad Z]^{\mathrm{T}}$, moments $[K \quad M \quad N]^{\mathrm{T}}$, linear velocities $[u \quad v \quad w]^{\mathrm{T}}$, and angular velocities $[p \quad q \quad r]^{\mathrm{T}}$ are usually expressed in

the body-fixed frame– see figure 1. We have used the standard notation given in SNAME (1950).

Let us define the position-orientation vector η with respect to the inertial frame as

$$\eta \triangleq \begin{bmatrix} x & y & z & \phi & \theta & \psi \end{bmatrix}^{\mathrm{T}} \tag{1}$$

and the linear-angular velocity vector ν with respect to the body-fixed frame as

$$\nu \triangleq \begin{bmatrix} u & v & w & p & q & r \end{bmatrix}^{\mathrm{T}} \tag{2}$$

Then, the position-orientation rate vector $\dot{\eta}$ is related to ν via:

$$\dot{\eta} = J(\eta)\,\nu\,, \tag{3}$$

where $J(\eta)$ is a transformation matrix that depends on the Euler angles $(\phi\,, \theta\,, \psi\ )$ and is of the form (Fossen, 1994):

$$J(\eta) = \begin{bmatrix} J_1(\phi\,, \theta\,, \psi) & \mathbf{0}_{3\times 3} \\ \mathbf{0}_{3\times 3} & J_2(\phi\,, \theta\,, \psi) \end{bmatrix} \tag{4}$$

where

$$J_1(\phi\,, \theta\,, \psi) = \begin{bmatrix} c(\psi)c(\theta) & -s(\psi)c(\phi) + c(\psi)s(\theta)s(\phi) & s(\psi)s(\phi) + c(\psi)c(\phi)s(\theta) \\ s(\psi)c(\theta) & c(\psi)c(\phi) + s(\phi)s(\theta)s(\phi) & -c(\psi)s(\phi) + s(\psi)c(\phi)s(\theta) \\ -s(\theta) & c(\theta)s(\phi) & c(\theta)c(\phi) \end{bmatrix} \tag{5}$$

and

$$J_2(\phi\,, \theta\,, \psi) = \begin{bmatrix} 1 & s(\phi)t(\theta) & c(\phi)t(\theta) \\ 0 & c(\phi) & -s(\phi) \\ 0 & s(\phi)/c(\theta) & c(\phi)/c(\theta) \end{bmatrix} \tag{6}$$

where $s(\cdot) = \sin(\cdot)$, $c(\cdot) = \cos(\cdot)$ and $t(\cdot) = \tan(\cdot)$.

Using the Newtonian approach, the equations of motion of vehicle in the body fixed frame are given in a vector form by:

$$\begin{aligned} M_{RB}\dot{\nu} &= \tau(\dot{\nu}, \nu, \eta) - C_{RB}(\nu)\nu \\ \dot{\eta} &= J(\eta)\nu, \end{aligned} \tag{7}$$

where M_{RB} is the matrix mass and inertia due to rigid body dynamics, the term $C_{RB}(\nu)\nu$ arise from the coriolis and centripetal forces and moments also due to rigid body dynamics, and $J(\eta)$ is given in (3). The forces and moments vector τ is defined as

$$\tau = \begin{bmatrix} X & Y & Z & K & M & N \end{bmatrix}^{\mathrm{T}}, \tag{8}$$

and these magnitudes are generated by different phenomena and can be separated into components according to their originating effects:

$$\tau = \tau_{hyd} + \tau_{cs} + \tau_{prop} + \tau_{ext}, \tag{9}$$

where

- *hyd*: These forces and moments arise from the movement of the hull in the water.
- *prop*: These forces and moments come from the propulsion system, e.g., propellers and thrusters.
- *cs*: These forces and moments arise due to the Control Surfaces (CS) like rudder, fins, etc. movement.
- *ext*: These are the forces and moments acting on the hull due to the environmental disturbances, e.g., wind, currents and waves.

Motions in pitch and heave can generally be neglected in comparison with the other motions for conventional surface ships; thus, ship motion modelling can be considered only 4-DOF: surge, sway, yaw and roll. Therefore, from (6) the following approximations can be made:

$$\dot{\phi} = p \qquad \dot{\psi} = rcos(\phi). \tag{10}$$

In the sequel we treat only the motion in four degrees of freedom (4-DOF.) For this case, the equations of motion (7) are

$$\begin{bmatrix} m & 0 & 0 & 0 \\ 0 & m & -mz_G & mx_G \\ 0 & -mz_G & I_{xx} & 0 \\ 0 & mx_G & 0 & I_{zz} \end{bmatrix} \begin{bmatrix} \dot{u} \\ \dot{v} \\ \dot{p} \\ \dot{r} \end{bmatrix} = \begin{bmatrix} X \\ Y \\ K \\ N \end{bmatrix} + \begin{bmatrix} m(vr + x_G r^2 - z_g pr) \\ -mur \\ mz_G ur \\ -mx_G ur \end{bmatrix}, \tag{11}$$

where m is mass of the ship, I_{xx} and I_{zz} are the inertias about the x_0 and z_0 axes, and x_G and z_G are the coordinates of the the center of gravity CG with respect to the body-fixed frame, *i.e.,* $\overline{CG} = [x_G,\, 0,\, z_G]$.

All the different force and moment components acting on the hull and their models shall be described in the following sections, except for the environmental disturbances that have been thoroughly treated for example in (Price and Bishop, 1974), (Blanke, 1981) and more recently in (Fossen, 1994).

3 Hydrodynamic forces and moments.

The hydrodynamic forces and moments can be studied by considering two problems. In the first, the movement of the hull when there are no incident waves is considered; while in the second one, the hull is restrained from moving and there are incident waves (Fossen, 1994). The second problem involves environmental forces like waves, wind and currents and is not considered here.

The hydrodynamic forces and moments arising from the first problem have dynamic and static origins and can be studied by analyzing different originating effects:

- *Motion in an ideal fluid with no circulation*: In this analysis, only the displacement is considered, and it reveals the so-called added mass and inertia forces and moments and Munk moment.

  The added mass and inertia reflects the build-up of kinetic energy of the fluid as the hull moves through it. The motion of the fluid associated with the accelerations produces the ship to move with an equivalent added mass and inertia, although the fluid do not move along with the ship. In the model, this effect is described by terms proportional to the accelerations.

  The Munk moment arise from the fact that in an ideal fluid, and elongated three-dimensional body at an angle of attack experiences a pure moment that tends to increase the angle of attack due to the change in direction of the fluid. This moment is composed of equal and opposite forces so there is no resultant force on the body (Lewis, 1988*c*). In the model, the Munk moment is described by terms proportional to the product of speeds uv.

- *Motion in an ideal fluid with circulation*: In this analysis the shape of the hull is relevant. For a body with a profile, like an air wing, there is a net force acting on it when it moves in the fluid with an angle of attack. This reveals the existence lift forces acting on the centre of preasure of the hull. Since the centre of preasure in sway motion is forward to the CG, there exist a moment that add to the Munk moment and tends to increase the angle of attack. The forces and moment are porportional to the products uv and ur.

- *Motion in a viscous fluid*: This analysis reveals the presence of hydrodynamic resistance. This resistance is made up of a number of different components caused by a variety if phenomena interacting in a very complex way. For instance, the total calm-water resistance can be assumed to be made up of three components (Lewis, 1988*b*):

  - The frictional resistance, due to the motion of the hull in viscous fluid.
  - The wave-making resistance, due to the energy carried away by the generated waves created on the surface.
  - Eddy resistance due to energy carried away by eddies shed from the hull and appendages.

  In the model, these effects are reflected by non-linearities of the kind $|u|u$, $|v|v$, $|r|v$, $|v|r$ and $|r|r$.

- *Gravitational and buoyancy forces*: These are the restoring forces and moments that depend on the Euler angles and act on the center of gravity CG and the center of buoyancy CB. These components can be considered as an equivalent to the spring forces in a mass-damper-spring system (Fossen, 1994).

The Hydrodynamic forces and moments are modelled as a nonlinear function of the accelerations $\dot{\nu}$, velocities ν, and the Euler angles included in η:

$$\tau_{hyd} = \mathbf{f}(\dot{\nu}, \nu, \eta),$$

and can be expressed in a series expansion that is affine in the parameters or coefficients. For example, for Y_{hyd} force:

$$Y_{hyd} \approx Y_{\dot{v}}\dot{v} + Y_{vv}v^2 + Y_{r|v|}r|v| + \dots \tag{12}$$

where the constant coefficients

$$Y_{\dot{v}} = \frac{\partial f_Y}{\partial \dot{v}} \qquad Y_{vv} = \frac{\partial^2 f_Y}{\partial v^2} \qquad Y_{r|v|} = \frac{\partial^2 f_Y}{\partial r \partial |v|}$$

are referred to as *hydrodynamic derivatives*. The first term in (12), for example, is interpreted as the force along the y_0-axis due to the acceleration $\dot{v}$ in the y_0-direction (see figure 1).

To determine the hydrodynamic derivatives, there are both theoretical methods like strip theory and experimental methods based on system identification and captive models. In the latter, a model is forced to move by a device called planar motion mechanism (PMM) (Goodman and Gertler, 1962). The PMM forces the body to move while the loads exerted on the model, positions, velocities and accelerations are measured. Analysis of the acquired data yields the values of the coefficients, see for example Jensen (1997).

We next review the model for the hydrodynamic forces of a container ship first presented in (Blanke and Jensen, 1997) and a multi-role naval vessel (Blanke *et al.*, 1989). These models were obtained using the four degrees of freedom Roll Planar Motion Mechanism (RPMM) facility at the Danish Maritime Institute.

3.1 Container hydrodynamic model

The structure of the RPMM model is shown below, in equations (15) to (19). The results are given as non-dimensional quantities using the *prime system* (SNAME, 1950)— see appendix A. In this model, the non-dimensional relative surge speed

$$u'_a \triangleq \frac{U - U_{nom}}{U} \tag{13}$$

is used in hydrodynamic terms, where U is the ship's absolute speed,

$$U \triangleq \sqrt{u^2 + v^2} \tag{14}$$

It should be noted that u'_a is different from non-dimensional surge velocity $u' = u/U$ which is involved when fictitious accelerations of equation 11 are calculated— see appendix A.

The non-dimensional relative surge speed is

$$\begin{aligned} X' = {} & X'_{\dot{u}}\dot{u}'_a + X'_u u'_a + X'_{uu}u'_a u'_a + X'_{uuu}u_a^{'3} \\ & + X'_{vr}v'r' + X'_{rr}r^{'2} \\ & + X'_v v' + X'_{vv}v^{'2} \\ & + X'_{v\phi}v'\phi' + X'_\phi \phi' + X'_{\phi\phi}\phi^{'2} \\ & + X'_{pp}p^{'2} + X'_{ppu}p^{'2}u'_a \end{aligned} \tag{15}$$

If the absolute speed is desired, a large signal model is employed instead where $X'(u')$ is the ship resistance, T' is the propeller thrust, and t is the thrust deduction factor (see section 4.)

$$\begin{aligned} X' = {} & X'_{\dot{u}}\dot{u}' + X'(u') + (1-t)T' + X'_{vr}v'r' + X'_{rr}r^{'2} + \\ & + X'_v v' + X'_{vv}v^{'2} \\ & + X'_{v\phi}v'\phi' + X'_\phi \phi' + X'_{\phi\phi}\phi^{'2} \\ & + X'_{pp}p^{'2} + X'_{ppu}p^{'2}u' \end{aligned} \tag{16}$$

The non-dimensional sway equation is

$$\begin{aligned} Y' = & Y'_{\dot{v}}\dot{v}' + Y'_{\dot{r}}\dot{r}' + Y'_{\dot{p}}\dot{p}' \\ & + Y'_{v}v' + Y'_{vv}v'^{2} + Y'_{v|v|}v'\,|v'| + Y'_{v|r|}v'\,|r'| + Y'_{vrr}v'r'^{2} \\ & + Y'_{r}r' + Y'_{r|r|}r'\,|r'| + Y'_{rrr}r'^{3} + Y'_{r|v|}r'\,|v'| + Y'_{rvv}rv'^{2} \\ & + Y'_{p}p' + Y'_{ppp}p'^{3} + Y'_{pu}p'u'_{a} + Y'_{pu|pu|}p'u'_{a}\,|p'u'_{a}| \\ & + Y'_{\phi}\phi' + Y'_{v\phi}v'\phi' + Y'_{v\phi\phi}v'\phi'^{2} + Y'_{\phi vv}\phi'v'^{2} + Y'_{0} + Y'_{0u}u'_{a} \end{aligned} \tag{17}$$

The non-dimensional roll equation is

$$\begin{aligned} K' = & K'_{\dot{p}}\dot{p}' + K'_{\dot{v}}\dot{v}' + K'_{\dot{r}}\dot{r}' \\ & + K'_{v}v' + K'_{vv}v'^{2} + K'_{v|v|}v'\,|v'| + K'_{v|r|}v'\,|r'| + K'_{vrr}v'r'^{2} \\ & + K'_{r|r|}r'\,|r'| + K'_{rrr}r'^{3} + K'_{rvv}r'v'^{2} + K'_{r|v|}r'\,|v'| \\ & + K'_{p}p' + K'_{p|p|}p'\,|p'| + K'_{ppp}p'^{3} + K'_{pu}p'u'_{a} + K'_{pu|pu|}p'u'_{a}\,|p'u'_{a}| \\ & + K'_{v\phi}v'\phi' + K'_{v\phi\phi}v'\phi'^{2} + K'_{\phi vv}\phi'v'^{2} \\ & + K'_{0} + K'_{0u}u'_{a} \\ & + K'_{r}\,r' - (\rho g \nabla G_{z}(\phi))' \end{aligned} \tag{18}$$

The non-dimensional yaw equation is

$$\begin{aligned} N' = & N'_{\dot{v}}\dot{v}' + N'_{\dot{r}}\dot{r}' + N'_{\dot{p}}\dot{p}' \\ & + N'_{v}v' + N'_{vv}v'^{2} + N'_{v|v|}v'\,|v'| + N'_{v|r|}v'\,|r'| + N'_{vrr}v'r'^{2} \\ & + N'_{r}r' + N'_{r|r|}r'\,|r'| + N'_{rrr}r'^{3} + N'_{rvv}r'v'^{2} + N'_{r|v|}r'\,|v'| \\ & + N'_{p}p' + N'_{ppp}p'^{3} + N'_{pu}p'u'_{a} + N'_{pu|pu|}p'u'_{a}\,|p'u'_{a}| \\ & + N'_{\phi}\phi' + N'_{v\phi}v'\phi' + N'_{v\phi\phi}v'\phi'^{2} + N'_{\phi vv}\phi'v'^{2} + N'_{0} + N'_{0u}u'_{a} \end{aligned} \tag{19}$$

where the last term of (18) corresponds to the restoring roll moment, in which ∇ denotes the ship displacement, g the gravity constant, ρ the mass density of the water and $G_z(\phi)$ is the buoyancy function for heel that can be approximated as (Lewis, 1988*a*),

$$G_z(\phi) = \left(GM + \frac{1}{2} BM \tan^2(\phi) \right) \sin(\phi) \tag{20}$$

where GM is the metacenter height, and BM is the distance from the center of buoyancy to the metacenter. The correct G_z curve is needed to get accurate results for large values of heel.

This ship was the first investigated with the RPMM experimental facility and subsequent experience from five later model tests have given certain amendments to finally yield the list of nonlinear hydrodynamic terms to cover a wider range of ship types (Blanke and Jensen, 1997).

3.2 Multi-role naval vessel hydrodynamic model

The structure of the RPMM model is shown below, in equations (21) to (25). The results are given in dimensional quantities.

The surge equation is

$$X = X_{\dot{u}}\dot{u} + X(u) + X_{vr}vr + (1-t)T, \tag{21}$$

where the resistance $X(u)$ is given by [1]

$$X(u) = X_{u|u|}u|u| \tag{22}$$

The sway equation is

$$\begin{aligned} Y = & Y_{\dot{v}}\dot{v} + Y_{\dot{r}}\dot{r} + Y_{\dot{p}}\dot{p} \\ & + Y_{|u|v}\,|u|\,v + Y_{ur}ur + Y_{v|v|}v\,|v| + Y_{v|r|}v\,|r| + Y_{r|v|}r\,|v| \\ & + Y_{\phi|uv|}\phi\,|uv| + Y_{\phi|ur|}\phi\,|ur| + Y_{\phi uu}\phi\,u^{2} \end{aligned} \tag{23}$$

[1] The RPMM test gave other terms; however, for this particular vessel, those terms are not available for publication.

The roll equation is

$$\begin{aligned} K = & K_{\dot{v}}\dot{v} + K_{\dot{p}}\dot{p} \\ & + K_{|u|v}\,|u|\,v + K_{ur}ur + K_{v|v|}v\,|v| + K_{v|r|}v\,|r| + K_{r|v|}r\,|v| \\ & + K_{\phi|uv|}\phi\,|uv| + K_{\phi|ur|}\phi\,|ur| + K_{\phi uu}\phi\,u^2 + K_{|u|p}\,|u|\,p \\ & + K_{p|p|}p\,|p| + K_p p + K_{\phi\phi\phi}\phi^3 - \rho g \nabla G_z(\phi) \end{aligned} \tag{24}$$

The yaw equation is

$$\begin{aligned} N = & N_{\dot{v}}\dot{v} + N_{\dot{r}}\dot{r} \\ & + N_{|u|v}\,|u|\,v + N_{|u|r}\,|u|\,r + N_{r|r|}r\,|r| + N_{r|v|}r\,|v| \\ & + N_{\phi|uv|}\phi\,|uv| + N_{\phi u|r|}\phi\,u\,|r| + N_{\phi u|u|}\phi\,u\,|u| \end{aligned} \tag{25}$$

This completes the non-linear hydrodynamic models.

4 Propulsion System and Resistance

In this section, we review the basic elements to model the propulsion effects and resistance. Let us consider as a propulsion device a propeller. The main task of the propeller system is the generation of available thrust T_a. This thrust is necessary to compensate the resistance forces $X(u)$ acting on the hull. Thus, in static conditions with the ship sailing at at a given forward speed in calm water, the resistance and the thrust balance, *i.e.,*

$$0 = X(u) + T_a \tag{26}$$

As previously mentioned, the resistance is made up of a number of different components caused by a variety if phenomena interacting in a very complex way. The simplest way to model the resistance effect is by a single term of the form

$$X(u) = X_{u|u|}u|u|. \tag{27}$$

An important effect produced when the ship moves in real fluid, is that the water around the stern acquires a forward motion in the direction of the motion of the hull. This forward-moving water is called the wake, and one of the effects it produces is a difference between the forward speed of the ship U and the average flow velocity over the propeller V_a, called the speed of advance. This difference, called the wake speed, is expressed as a fraction of the speed U as,

$$w = \frac{U - V_a}{U}$$

and

$$V_a = (1 - w)U \tag{28}$$

The wake fraction is determined by a combination of propulsion tests to derive the thrust and the use of the open water propeller characteristics– see (Lewis, 1988*b*). The wake is generally positive in the majority of the cases. Exceptions occur in high speed vessels, like destroyers and power boats, in which the wave pattern generated at high speed presents a through at stern. In those cases the wake could either be zero or negative (Lewis, 1988*b*).

There is another important effect due to the interaction between propeller and hull. When the ship is towed, there is an area of high pressure over the stern which reduces the total resistance since it partly compensates forces produced by the high pressure area in the bow. With a self-propelled hull, the pressure over some of the area over the stern is reduced due to the propeller action that accelerates the water, thus the resistance is increased and so the trust necessary to move the ship. The common practice it to view this increase in resistance as a deduction from the thrust generated by the propeller. This is described by a thrust deduction number t— typically 0.05-0.2 (Fossen, 1994)— such that the thrust available for the propulsion is

$$T_a = (1 - t)T\,, \tag{29}$$

where T is the propeller generated thrust. This available thrust may be regarded as independent of ship speed.

5 Rudder forces and moments

In this section, we give a model to calculate the force on the rudder, and then according to its position and orientation on the hull, geometrically relate this force to the generated forces and moments that produce motion of the ship. The results can be generalized to any moving fin.

5.1 Modelling using physical laws

The total resulting hydrodynamic force acting on the rudder in a real fluid acts on a single point on the rudder called center of pressure CP with coordinates $\overline{CP} = [x_{cp} \quad y_{cp} \quad z_{cp}]^{\mathrm{T}}$ expressed in the fixed body frame . In contrast to the resultant force described by two-dimensional wing theory, in which the force would be normal to the direction of the flow, the total resultant force in a real fluid is nearly normal to the center plane of the rudder (Lewis, 1988*b*). The magnitude of resulting force considered normal to the rudder can be expressed as

$$F = \begin{cases} \frac{1}{2}\rho C_F A_r V_{av}^2 sin(\frac{\pi}{2}\frac{\delta_{attack}}{\delta_{stall}}) & \text{if } |\delta_{attack}| < \delta_{stall}\,, \\ \frac{1}{2}\rho C_F A_r V_{av}^2 sign(\delta_{attack}) & \text{if } |\delta_{attack}| \geq \delta_{stall}\,, \end{cases} \tag{30}$$

where C_F is the lift coefficient, A_r is the rudder area, V_{av} is the average flow passing the rudder and δ_{stall} is the rudder stall angle. The angle of attack δ_{attack} is the relative angle between the rudder and the flow. This angle is calculated using the rudder angle δ the sway velocity v, the surge velocity u and the sway velocity at stern produced by the turn rate of the ship $(x_{cp} - x_G)r$ as

$$\begin{aligned} \delta_{attack} &= \delta - \delta_{flow} \\ &= \delta - \arctan(\frac{v + (x_{cp} - x_G)r}{u}), \end{aligned} \tag{31}$$

where the magnitudes are according to the adopted convention (SNAME, 1950), see figure 2. The forces due

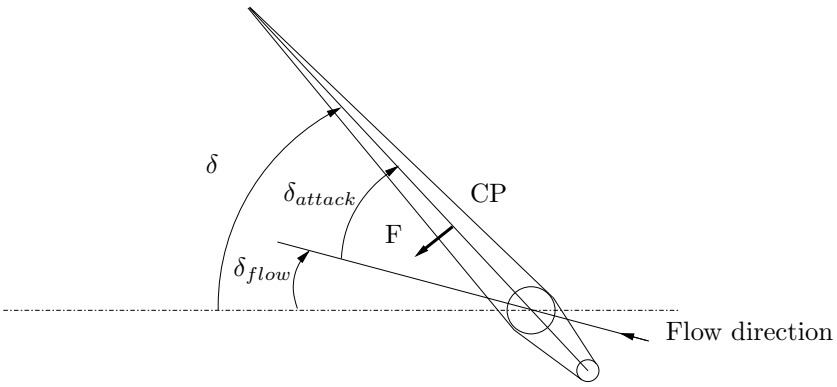

Figure 2: Rudder angles definition and convension.

to the rudder acting on the hull are then given

$$\begin{aligned} X_{rudder} &= -F(u, V_{av}, , v, r, \delta)\sin(\delta), \\ Y_{rudder} &= F(u, V_{av}, v, r, \delta)\cos(\delta), \\ Z_{rudder} &= 0. \end{aligned} \tag{32}$$

and the moments are

$$[K_{rudder} \quad M_{rudder} \quad N_{rudder}]^{\mathrm{T}} = (\overline{CP} - \overline{CG}) \times [X_{rudder} \quad Y_{rudder} \quad Z_{rudder}]^{\mathrm{T}}. \tag{33}$$

Since the rudder is located behind the propeller, the flow passing the rudder V_{av} is very much influenced by the propeller. van Berlekom (1975) proposed a series of models test and expressed the average flow as

$$V_{av}^2 = V_a^2 + C_T T, \tag{34}$$

where

$$C_T \approx \frac{6.4}{\pi\rho h D_p},$$

in which h is the rudder span and D_p is the propeller diameter. Using the static condition between effective thrust and resistance (26) together with (28) and (34), V_{av} can be expressed as

$$V_{av}^2 = \left[(1-w)^2 - C_T^2 \frac{X_{uu}}{(1-t)}\right] U^2. \tag{35}$$

5.2 Generalization to any fin

The results presented in the previous section can be generalized to any fin by proper geometrical relations. The forces acting on the fin, can be expressed in a fin reference frame. This frame is defined with origin in the CP, and it moves with the CP mantainig its orientation. The orientation of the fin frame is defined when the relative angle between the fin and the flow is zero by rotating the body-fixed frame an angle θ_{tilt} about the unitary vector $\lambda = [\lambda_1 \quad \lambda_2 \quad \lambda_3]^{\mathrm{T}}$. For example, a centered rudder will be described by: $\overline{CP} = [x_{cp} \quad 0 \quad z_{cp}]^{\mathrm{T}}$, $\lambda = [1 \quad 0 \quad 0]^{\mathrm{T}}$ and $\theta_{tilt} = 0$, while a horizontal stabilizing fin on the starboard side by: $\overline{CP} = [x_{cp} \quad y_{cp} \quad z_{cp}]^{\mathrm{T}}$, $\lambda = [1 \quad 0 \quad 0]^{\mathrm{T}}$ and $\theta_{tilt} = -\pi/2$. The forces on the fin frame are given by

$$\begin{aligned} X_f &= -F\sin(\delta_r), \\ Y_f &= F\cos(\delta_r), \\ Z_f &= 0, \end{aligned} \tag{36}$$

where F is given by a similar form of expression (30). We say 'in a similar form' since depending on the position of the fin, other components of motion like roll may be considered to determine the angle of attack.

The forces acting on the center of gravity are obtained via the following rotation matrix (Fossen, 1994):

$$[X \quad Y \quad Z]^{\mathrm{T}} = Rot(\lambda, \theta_{tilt})[X_f \quad Y_f \quad Z_f]^{\mathrm{T}}, \tag{37}$$

where

$$Rot(\lambda, \theta_{tilt}) = \cos(\theta_{tilt})\mathbf{I} + (1 - \cos(\theta_{tilt}))\lambda\lambda^{\mathrm{T}} - \sin(\theta_{tilt})\mathbf{S}(\lambda) \tag{38}$$

and

$$\mathbf{S}(\lambda) \triangleq \begin{bmatrix} 0 & -\lambda_3 & \lambda_2 \\ \lambda_3 & 0 & -\lambda_1 \\ -\lambda_2 & \lambda_1 & 0 \end{bmatrix} \tag{39}$$

Finally, the moments are given by

$$[K \quad M \quad N]^{\mathrm{T}} = (\overline{CP} - \overline{CG}) \times [X \quad Y \quad Z]^{\mathrm{T}}. \tag{40}$$

5.3 RPMM rudder forces model

Another option to model the forces and moment produced by the rudder is to use the RPMM facility to obtain this model. For example, for the container ship we have (Blanke and Jensen, 1997)

$$\begin{aligned} X_{rudder} &= X'_{\delta}\delta' + X'_{\delta\delta}\delta'^2 + X'_{\delta u}\delta' u'_a + X'_{\delta\delta u}\delta'^2 u'_a \\ &\quad + X'_{v\delta}v'\delta' + X'_{v\delta\delta}v'\delta'^2 \\ Y_{rudder} &= Y'_{\delta}\delta' + Y'_{\delta\delta}\delta'^2 + Y'_{\delta\delta\delta}\delta'^3 \\ &\quad + Y'_{\delta v}\delta'v' + Y'_{\delta vv}\delta'v'^2 + Y'_{\delta u}\delta'u'_a + Y'_{\delta\delta u}\delta'^2 u'_a + Y'_{\delta\delta\delta u}\delta'^3 u'_a \\ K_{rudder} &= K'_{\delta}\delta' + K'_{\delta\delta}\delta'^2 + K'_{\delta\delta\delta}\delta'^3 \\ &\quad + K'_{\delta v}\delta'v' + K'_{\delta vv}\delta'v'^2 + K'_{\delta u}\delta'u'_a + K'_{\delta\delta u}\delta'^2 u'_a + K'_{\delta\delta\delta u}\delta'^3 u'_a \\ N_{rudder} &= N'_{\delta}\delta' + N'_{\delta\delta}\delta'^2 + N'_{\delta\delta\delta}\delta'^3 \\ &\quad + N'_{\delta v}\delta'v' + N'_{\delta vv}\delta'v'^2 + N'_{\delta u}\delta'u'_a + N'_{\delta\delta u}\delta'^2 u'_a + N'_{\delta\delta\delta u}\delta'^3 u'_a \,. \end{aligned} \tag{41}$$

6 Rudder Machinery

The mathematical model of the rudder mechanism most commonly used in computer simulations and autopilot design is the simplified model presented by van Amerongen (1982). In figure 3, we see a block diagram representation of the model. This model captures the essential effects produced by the rudder machinery:

- Magnitude saturation: the rudder motion is constrained to move within certain maximum angles, *i.e.,* $-\delta_{max} \leq \delta \leq \delta_{max}$ (rad).
- Slew rate saturation: The rate of rudder movement is limited by a maximum value $\dot{\delta}_{max}$ (rad/sec).

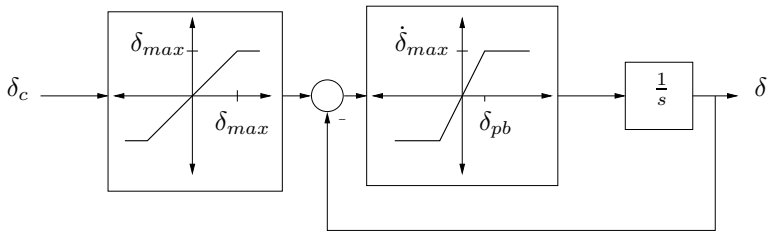

Figure 3: Simplified block diagram of the steering machine model.

- Time delay: the main servo is the responsible of producing most of the delay between the ruder command δ_c and the actual rudder angle δ. In the linear zone, the delay is represented by a first order system with a time constant

$$\tau_\delta = \frac{\dot{\delta}_{max}}{\delta_{pb}}$$

where δ_{pb} is the so-called proportional band.

7 Non-linear and linearized state space models

7.1 Non-linear models

The non-linear state space models are based on (11), and the models for the forces and moments given in the previous sections. The non-linear state space model has the general form

$$\dot{x} = H^{-1} f(x, \delta)\,. \tag{42}$$

where

$$x = \begin{bmatrix} u & v & r & p & \phi & \psi \end{bmatrix}^{\mathrm{T}}\,, \tag{43}$$

The model (42) can be treated either in a dimensional or non-dimensional manner according the given hydrodynamic model. A special care should be taken when when using models with the normalized variable u'_a given in (13) and u' together as we will show in this section. We now describe the elements of (42).

Incorporating the time derivatives of the roll and yaw angles given in (10), Newton's equations of motion given in (11) can be re arranged as follows

$$\begin{aligned}
(m - X_{\dot{u}})\dot{u} &= X^*_{hyd}(x) + X_{rudder}(x,\delta) + m(vr + x_G r^2 - z_G pr) \\
(m - Y_{\dot{v}})\dot{v} - (mz_G + Y_{\dot{p}})\dot{p} + (mx_G - Y_{\dot{r}})\dot{v} &= Y^*_{hyd}(x) + Y_{rudder}(x,\delta) - mur \\
-(mz_G + K_{\dot{v}})\dot{v} + (I_{xx} - K_{\dot{p}})\dot{p} - K_{\dot{r}}\dot{p} &= K^*_{hyd}(x) + K_{rudder}(x,\delta) + mz_G ur \\
(mx_G - N_{\dot{v}})\dot{v} - N_{\dot{p}}\dot{p} + (I_{zz} - N_{\dot{r}})\dot{r} &= N^*_{hyd}(x) + N_{rudder}(x,\delta) - mx_G ur \\
\dot{\phi} &= p \\
\dot{\psi} &= r\cos(\phi)
\end{aligned} \tag{44}$$

where the terms $X^*_{hyd}(x)$ $Y^*_{hyd}(x)$, $K^*_{hyd}(x)$ and $N^*_{hyd}(x)$ correspond to the hydrodynamic models given in section 3 and are either the set of equations (15) to (19) or (21) to (25) without the terms that proportional to the accelerations. The matrix H is given by

$$H = \begin{bmatrix}
(m - X_{\dot{u}}) & 0 & 0 & 0 & 0 & 0 \\
0 & (m - Y_{\dot{v}}) & -(mz_G + Y_{\dot{p}}) & (mx_G - Y_{\dot{r}}) & 0 & 0 \\
0 & -(mz_G + K_{\dot{v}}) & (I_{xx} - K_{\dot{p}}) & -K_{\dot{r}} & 0 & 0 \\
0 & (mx_G - N_{\dot{v}}) & -N_{\dot{p}} & (I_{zz} - N_{\dot{r}}) & 0 & 0 \\
0 & 0 & 0 & 0 & 1 & 0 \\
0 & 0 & 0 & 0 & 0 & 1
\end{bmatrix} \tag{45}$$

and

$$f(x,\delta) = \begin{bmatrix} X^*_{hyd}(x) + X_{rudder}(x,\delta) + m(vr + x_G r^2 - z_G pr) \\ Y^*_{hyd}(x) + Y_{rudder}(x,\delta) - mur \\ K^*_{hyd}(x) + K_{rudder}(x,\delta) + mz_G ur \\ N^*_{hyd}(x) + N_{rudder}(x,\delta) - mx_G ur \\ p \\ r\cos(\phi) \end{bmatrix} \tag{46}$$

When we consider a non-dimensional model in which the state is given by $x' = \begin{bmatrix} u'_a & v' & r' & p' & \phi' & \psi' \end{bmatrix}^{\mathrm{T}}$, expression (46) should be modified as follows

$$f'(x',\delta') = \begin{bmatrix} X'^*_{hyd}(x') + X'_{rudder}(x',\delta') + m'(v'r' + x'_G r'^2 - z'_G p'r') \\ Y^{*\prime}_{hyd}(x') + Y_{rudder}(x',\delta') - m'h'(x',u'_a)r' \\ K^{*\prime}_{hyd}(x') + K'_{rudder}(x',\delta') + m'z'_G h'(x',u'_a)r' \\ N^{*\prime}_{hyd}(x') + N'_{rudder}(x',\delta') - m'x'_G h'(x',u'_a)r' \\ p' \\ r'\cos(\phi') \end{bmatrix}, \tag{47}$$

where we have used the following relations

$$U = \frac{U_{nom}}{(1 - u_a\prime)} \tag{48}$$

and

$$u' = h'(x',u'_a) = \frac{1}{U}\sqrt{\frac{U^2_{nom}}{(1-u'_a)^2} - (U_{nom}v')^2} \tag{49}$$

that has been derived from the definitions of u'_a (*cf.,* (13)) and u' (see appendix A).

7.2 Linearized models

It is a common practice to decouple the surge equation from the others to analyze the linearized models. Thus, we consider a given service speed $\overline{u}$ (or the approximation $\overline{u}'_a \approx (\overline{u} - U_{nom})/U_{nom}$) and the reduced state vector $z = \begin{bmatrix} v & r & p & \phi & \psi \end{bmatrix}^{\mathrm{T}}$.The linearized models are obtained straightforward from (42) as

$$\begin{aligned} \dot{z} &= H^{-1}\left[\left.\frac{\partial f(z,u,\delta)}{\partial z}\right|_{\overline{z},\overline{u},\overline{\delta}} \quad z + \left.\frac{\partial f(z,u,\delta)}{\partial \delta}\right|_{\overline{z},\overline{u},\overline{\delta}} \quad \delta \right] \\ &= H^{-1}A \quad z + M^{-1}B \quad \delta. \end{aligned} \tag{50}$$

The matrix H is now given by (45) without the first row and first column, and to obtain the matrices A and B, the Jacobians in (50) are evaluated at $\overline{z} = [0 \quad 0 \quad 0 \quad 0 \quad 0]^{\mathrm{T}}$ and $\overline{\delta} = 0$.

For the container ship, from (15) to (19) and from the RPMM rudder model (41), the non-dimensional matrices F and G are are as follows

$$A = \begin{bmatrix} Y'_v & Y'_p + Y'_{pu}\overline{u}'_a & Y'_r - m'\overline{u}' & Y'_\phi & 0 \\ K'_v & K'_p + K'_{pu}\overline{u}'_a & K'_r + m'z'_G\overline{u}' & -(\rho g \nabla GM)' & 0 \\ N'_v & N'_p + N'_{pu}\overline{u}'_a & N'_r + m'z'_G\overline{u}' & N'_\phi & 0 \\ 0 & 1 & 0 & 0 & 0 \\ 0 & 0 & 1 & 0 & 0 \end{bmatrix}, \quad B = \begin{bmatrix} Y'_\delta \\ K'_\delta \\ N'_\delta \\ 0 \\ 0 \end{bmatrix}. \tag{51}$$

The naval vessel has two rudders, and their effect is accounted using the model obtained by physical laws presented in section 5. Therefore, we have

$$A = \left.\frac{\partial f_{hyd}(z,u,\delta)}{\partial z}\right|_{\overline{z},\overline{u},\overline{\delta}} + \left.\frac{\partial f_{rudder}(z,u,V_{av},\delta)}{\partial z}\right|_{\overline{z},\overline{u},\overline{V}_{av},\overline{\delta}} \tag{52}$$

$$B = \left.\frac{\partial f_{rudder}(z,u,V_{av},\delta)}{\partial \delta}\right|_{\overline{x},\overline{u},\overline{V}_{av},\overline{\delta}}, \tag{53}$$

where in the function $f_{hyd}(z,u,\delta)$, we have included the terms corresponding to the coriolis and centripetal accelerations. Then from (23) to (25), and (46) we obtain

$$\left.\frac{\partial f_{hyd}(z,u,\delta)}{\partial z}\right|_{\overline{z},\overline{u},\overline{\delta}} = \begin{bmatrix} Y_{|u|v}|\overline{u}| & 0 & (Y_{ur}-m)\overline{u} & Y_{\phi uu}\overline{u}^2 & 0 \\ K_{|u|v}|\overline{u}| & K_p + K_{|u|p}|\overline{u}| & (K_{ur}+mz_G)\overline{u} & K_{\phi uu}\overline{u}^2 - \rho g \nabla GM & 0 \\ N_{|u|v}|\overline{u}| & 0 & N_{|u|r}|\overline{u}| - mx_G\overline{u} & N_{\phi u|u|}\overline{u}|\overline{u}| & 0 \\ 0 & 1 & 0 & 0 & 0 \\ 0 & 0 & 1 & 0 & 0 \end{bmatrix}. \tag{54}$$

To simplify the linear model of the rudder, we assume that the rudders has no tilt angle (they have a tilt angle of $6deg$, see appendix C), and that the angle of attack is small. Under these assumptions, we obtain

$$\left.\frac{\partial f_{rudder}(z,u,V_{av},\delta)}{\partial z}\right|_{\overline{z},\overline{u},\overline{V}_{av},\overline{\delta}} = \frac{Y_{\delta uu}\overline{V}_{av}^2}{\overline{u}} \begin{bmatrix} -1 & 0 & (x_{cp}-x_G) & 0 & 0 \\ (z_{cp}-z_G) & 0 & (z_{cp}-z_G)(x_{cp}-x_G) & 0 & 0 \\ -(x_{cp}-x_G) & 0 & -(x_{cp}-x_G)(x_{cp}-x_G) & 0 & 0 \\ 0 & 0 & 0 & 0 & 0 \\ 0 & 0 & 0 & 0 & 0 \end{bmatrix}, \tag{55}$$

$$\left.\frac{\partial f_{rudder}(z,u,V_{av},\delta)}{\partial \delta}\right|_{\overline{z},\overline{u},\overline{V}_{av},\overline{\delta}} = \begin{bmatrix} Y_{\delta uu}\overline{V}_{av}^2 \\ -(z_{cp}-z_G)Y_{\delta uu}\overline{V}_{av}^2 \\ (x_{cp}-x_G)Y_{\delta uu}\overline{V}_{av}^2 \\ 0 \\ 0 \end{bmatrix}, \tag{56}$$

and

$$Y_{\delta uu} = \frac{\pi \rho C_F A_r}{4 \quad \delta_{stall}}.$$

8 Simulation results

8.1 Response to different rudder commands

In this section, we present some simulation results using the given models for the naval vessel and the container ship. In the simulations, we perform two different tests. In the first test, a step of 10 deg is applied in the rudder towards port, while in the second, a sinusoidal rudder command is applied. In the later, the period of the sinusoidal is varied linearly between values close to the roll natural period so as to excite the roll modes. The roll natural period of the ship is estimated by

$$T_0 = 2\pi\sqrt{\frac{I_{zz} - K_{\dot{p}}}{\rho g \nabla GM}}.$$

In figure 4, we can see the response of the states for the linear (dash-dot) and non-linear (cont.) models. The non linear model has been validated via full-scale trials; however, in this report only the parameters at a project stage are given in the appendix C. In figure 5, we can see the response of both models for the sinusoidal rudder command with linearly varying frequency.

From figures 4 and 5 it can be appreciated that the linear model performs well in general. The response shown in figure 4 depicts a small difference between the linear and non-linear models at low frequencies. Other simulation results, not shown here, indicate that the cause of this difference can neither be considered due to the linearization of the hydrodynamic nor the rudder models alone, but a combination of both. Specifically, the particular kind of non-linearities of the form $v|r|$, $r|r|$, $v|v|$ and the like not described by the linear approximation in hydrodynamic model and the non linear effect of the rudder combined are the cause of this differences in response at low frequency.

In figures 6 and 7, we can see the results of the same type of tests for the container ship model. Similar comments to the ones made for the naval vessel apply to this model. In this case, the linear model has stable pole at very low frequency that produce a significant difference at low frequencies. Nevertheless, the performance of the linear model at high frequency is deemed satisfactory.

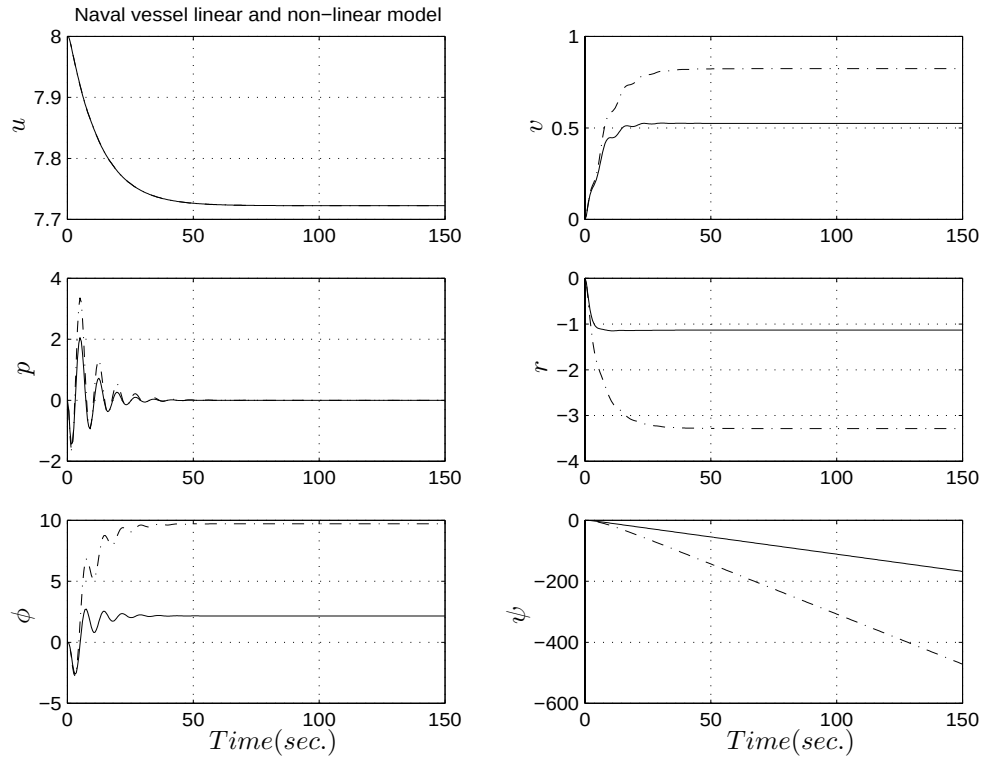

Figure 4: Response of linear (dash-dot) and non-linear (solid) models for a naval vessel for a 10 deg port rudder step.

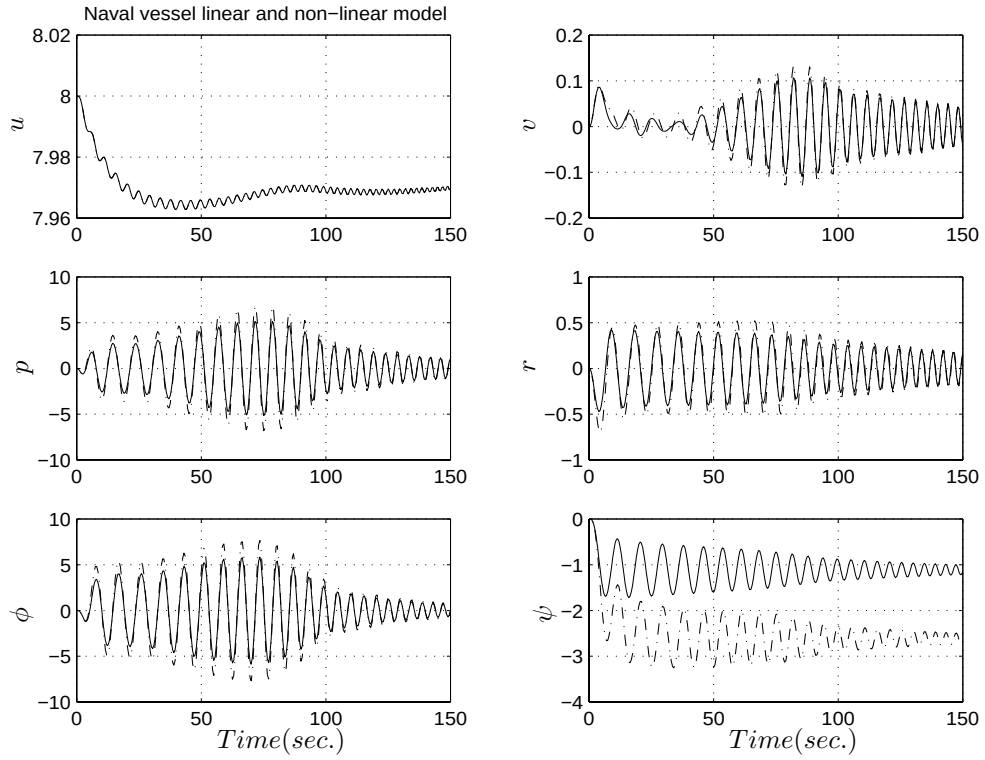

Figure 5: Response of linear (dash-dot) and non-linear (solid) models for a naval vessel for a 5 deg chirp signal rudder command.

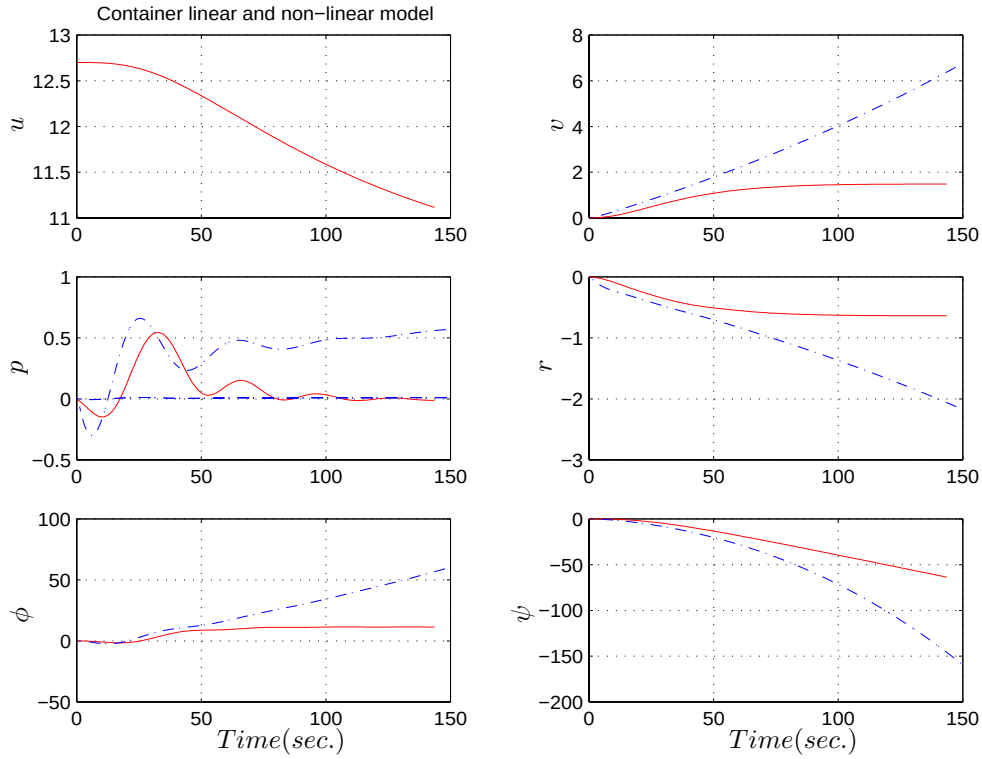

Figure 6: Response of linear (dash-dot) and non-linear (solid) models for a container ship for a 10 deg port rudder step.

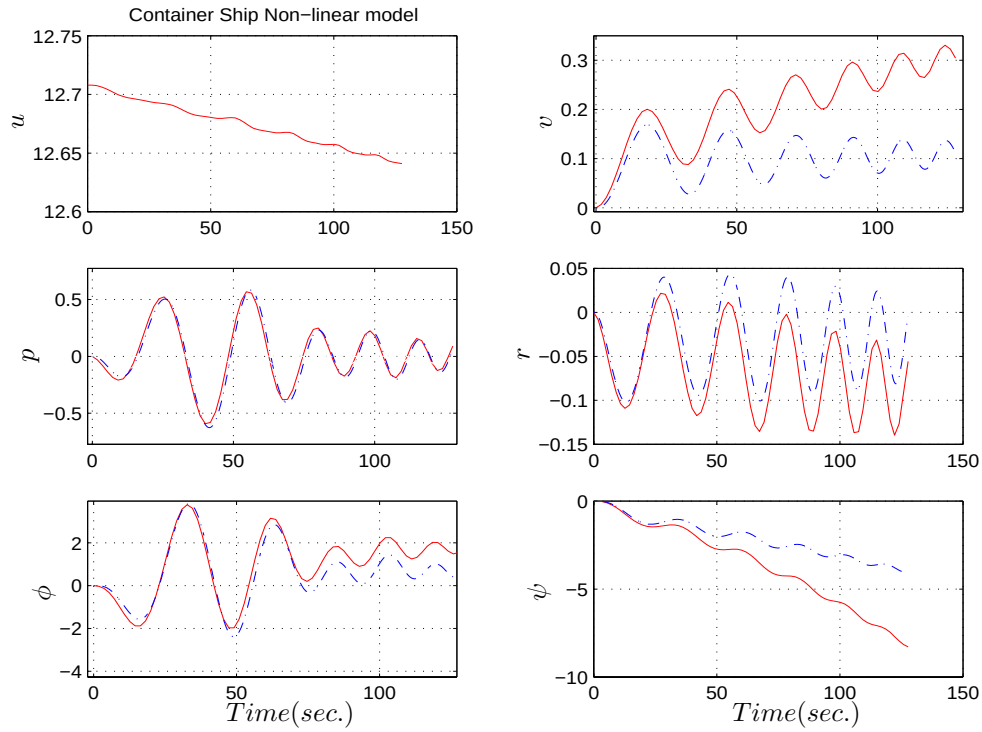

Figure 7: Response of linear (dash-dot) and non-linear (solid) models for a container ship for a 5 deg chirp signal rudder command..

8.2 Parameter sensitivity study

In this section, we perform a study of sensitivity via numerical simulation. Specifically, we perform single parameter variations for the non-linear state space model of the naval vessel. To evaluate the sensitivity of the model, we define the following sensitivity cost functionals

$$J_{roll}(\tilde{\theta}) = \left| 100 \frac{\sum_{t=0}^{N} p(t,\tilde{\theta})^2 + \phi(t,\tilde{\theta})^2 - \sum_{t=0}^{N} p(t,\theta)^2 + \phi(t,\theta)^2}{\sum_{t=0}^{N} p(t,\theta)^2 + \phi(t,\theta)^2} \right|, \tag{57}$$

$$J_{steering}(\tilde{\theta}) = \left| 100 \frac{\sum_{t=0}^{N} v(t,\tilde{\theta})^2 + r(t,\tilde{\theta})^2 - \sum_{t=0}^{N} v(t,\theta)^2 + r(t,\theta)^2}{\sum_{t=0}^{N} v(t,\theta)^2 + r(t,\theta)^2} \right|, \tag{58}$$

where for example, $p(t,\tilde{\theta})$ is the time response of the roll rate when the perturbed parameter value $\tilde{\theta}$ with respect to the original parameter value θ is is used, and N is the simulation time. The use of two different functions separating the roll part from the steering part allows us to evaluate the sensitivity of the couplings between roll, sway and yaw.

In the first test, a step signal of $10deg$ is applied in the rudder command, and the simulation is done for a period of time of $150sec$. All the parameters in the non-linear models are varied -50%, -10%, $+10\%$, $+50\%$ from its nominal values. The results are shown in table 1.

	J_{roll}		$J_{steering}$	
Parameter	$\pm 50\%$	$\pm 10\%$	$\pm 50\%$	$\pm 10\%$
$N_{\|u\|v}$	61	11	8	1.5
$N_{\|u\|r}$	200	23	23	3
$N_{r\|r\|}$	12	2	2	0.3
$K_{r\|v\|}$	26	4	4	1
$N_{\phi\|uv\|}$	0.2	0.05	0.05	0.01
$N_{\phi u\|r\|}$	3	0.7	0.5	0.1
$N_{\phi u\|u\|}$	2	0.4	0.3	0.07
$K_{\|u\|v}$	40	7	2	0.3
K_{ur}	15	3	0.7	0.1
$K_{v\|v\|}$	7	1	0.3	0.07
$K_{v\|r\|}$	6	1	0.3	0.06
$K_{r\|v\|}$	1	0.3	0.06	0.01
$K_{\phi\|uv\|}$	1	0.2	0.05	0.01
$K_{\phi\|ur\|}$	1	0.2	0.05	0.01
$K_{\phi uu}$	3	0.5	0.1	0.02
$K_{\|u\|p}$	1.5	0.2	0.01	0.001
$K_{\|p\|p}$	0.1	0.02	0.001	0.0001
K_p	2	0.3	0.01	0.002
$K_{\phi\phi\phi}$	0.06	0.001	0.003	0.0006
$Y_{\|u\|v}$	90	11	100	13
Y_{ur}	20	4	30	5
$Y_{v\|v\|}$	1	0.2	1	0.3
$Y_{v\|r\|}$	9	2	11	2
$Y_{r\|v\|}$	2	0.4	2	0.5
$Y_{\phi\|uv\|}$	1.5	0.3	2	0.5
$Y_{\phi\|ur\|}$	1.3	0.2	2	0.3
$Y_{\phi uu}$	0.1	0.03	0.2	0.04

Table 1: Sensitivity to a single parameter variation for a $10deg$ step rrudder command and $150sec$ simulation time.

In the second test, we use a sinusoidal rudder command of amplitude $5deg$ with a period varying linearly from $10sec$ to $6sec$ in $150sec$. The results are shown in Table 2.

Parameter	J_{roll} ±50%	±10%	$J_{steering}$ ±50%	±10%
$N_{\|u\|v}$	0.4	0.07	1.5	0.3
$N_{\|u\|r}$	33	5	21	2
$N_{r\|r\|}$	0.7	0.1	0.4	0.07
$K_{r\|v\|}$	0.2	0.05	0.2	0.03
$N_{\phi\|uv\|}$	0.7	0.1	0.5	0.1
$N_{\phi u\|r\|}$	1.4	0.2	0.8	0.1
$N_{\phi u\|u\|}$	3	0.5	2	0.4
$K_{\|u\|v}$	3.5	0.6	5	1
K_{ur}	0.6	0.1	1	0.2
$K_{v\|v\|}$	0.1	0.02	0.1	0.03
$K_{v\|r\|}$	0.07	0.01	0.1	0.02
$K_{r\|v\|}$	0.005	0.001	0.0001	0.00002
$K_{\phi\|uv\|}$	0.004	0.001	0.02	0.004
$K_{\phi\|ur\|}$	0.01	0.003	0.1	0.01
$K_{\phi uu}$	0.8	0.1	0.4	0.1
$K_{\|u\|p}$	9	2	8	1.5
$K_{\|p\|p}$	2	0.3	2	0.3
K_p	46	7	43	6
$K_{\phi\phi\phi}$	0.03	0.001	0.08	0.01
$Y_{\|u\|v}$	2.5	0.5	9	2
Y_{ur}	1.6	0.3	1	0.1
$Y_{v\|v\|}$	0.007	0.001	0.02	0.004
$Y_{v\|r\|}$	0.06	0.01	0.2	0.04
$Y_{r\|v\|}$	0.01	0.002	0.02	0.004
$Y_{\phi\|uv\|}$	0.04	0.01	0.2	0.04
$Y_{\phi\|ur\|}$	0.2	0.04	0.5	0.1
$Y_{\phi uu}$	0.1	0.03	0.4	0.08

Table 2: Sensitivity to a single parameter variation for a sinusoidal rudder command on $150sec$ simulation time.

From Table 1 and Table 2, we appreciate that the non-linear model for the naval vessel is very sensitive to some parametes, especially when it is exited at low frequency. At low frequency, the parameters with larger sensitivity are

$$N_{|u|v}, \quad N_{|u|r}, \quad N_{r|v|}, \quad K_{|u|v}, \quad K_{ur}, \quad Y_{|u|v}, \quad Y_{ur}. \tag{59}$$

There is no significant sensitivity to parameters accounting roll motion since the roll modes are not being excited.

Results from Table 2, show that the sensitivity of the model at high frequency is, in general, less than at low frequency. However, the sensitivity of $N_{|u|r}$ is still significant, and since in the second test the roll models are exited, the sensitivity to K_p is significant, not only to the roll but also to the steering.

9 Summary and discussion

In this report, we have reviewed the models for describing the motion of the ship in four degrees of freedom. Non-linear hydrodynamic models obtained from tests at the RPMM facility at the Danish Maritime Institute and then validated via extensive full scale trials were presented. From the non-linear hydrodynamic models, state space models both non-linear and linearized, in surge, sway, roll and yaw were obtained.

The non-linear models describe the dynamic response of the ships very accurately, and therefore can be utilized at first stage for testing control strategies. Similarly, the linear models presented are preferred for control application design to models obtained from system identification, and other models presented in the literature (see for example (van der Klugt, 1987)) since they reveal explicit dependency with the speed of

operation and thus can be easily up-dated for different speeds.

Simulation results with fully parameterized models for a container ship and a naval vessel were used to access the quality of the linearized models. The linear models perform well at high frequency, *i.e.,* frequencies in the range of the natural roll frequency, but their behavior departs from the non-linear counter parts at low frequencies. This effect is negligible for the naval vessel, but significant for the container ship. No general conclusions can be drawn since the RPMM models vary from ship to ship, and thus the quality of the linearized model. For some particular ships, and applications, it should be considered using linear models fitted at different frequencies. For example, a rudder-roll-damping model-based autopilot design requires a model that works well at frequencies close to the roll natural frequency.

Simple sensitivity analysis via numerical simulation was done for the non-linear model of the naval vessel. This study reveals that the model is generally insensitive to single parameter variations at high frequency; however, at low frequency there are some parameters for which the sensitivity results one order of magnitude bigger than for the rest of the parameters. Some of this parameters are present in the linearized models, and therefore their variation should also be reflected in the linearized model behavior. This analysis provides an indication of which parameters are more important to be identified to tune the models for implementing any model-based control strategy.

References

Abkowitz, M.A. (1975). Lectures on ship hydrodynamics- steering and manoeuvrability. Technical Report Rep. No. Hy-5. Hydro og Aerodynamisk Laboratorium, Lyngby, Denmark.

Blanke, M. and A. Christensen (1993). Rudder roll dumping autopilot robustness to sway-yaw-roll couplings. *In: Proceedings of 10th SCSS, Ottawa, Canada* pp. 93–119.

Blanke, M. and A.G. Jensen (1997). Dynamic properties of container vessel with low metacentric height. Technical Report doc. No. R-1997-4173. Dept. of Control Engineering, Aalborg University, Denmark.

Blanke, M., P. Haals and K.K. Andreasen (1989). Rudder roll damping experience in denmark. In: *Proceedings of IFAC work shop CAMS'89, Lyngby, Denmark.*

Blanke, Mogens (1981). Ship propulsion losses related to automatic steering and prime mover control. PhD thesis. Servolaboratory, Tecnical University of Denmark.

Chislett, M.S. (1990). The addition of heel-roll servo mechanism to the dmi horizontal planar motion mechanism. In: *Proc. of MARSIM and ICSM, Tokio, Japan.*

Chislett, M.S. and J. Støm-Tejsen (1965). Planar motion mechanism tests and full scale steering and maneuvering predictions of a mariner class vessel. Technical Report Rep. No. Hy-6. Hydro og Aerodynamisk Laboratorium, Lyngby, Denmark.

Fossen, Thor I. (1994). *Guidance and Control of Ocean Marine Vehicles.* John Wiley and Sons Ltd. New York.

Goodman, A. and M. Gertler (1962). Planar motion mechanism system. US patent 3052120.

Jensen, Andreas G. (1997). Fluid dynamic derivatives: marine and wind engineering approaches. *Journal of Wind Eng. and Industrial Aerodynamics* **69**(71), 777–793.

Kälström, C.G. and P. Otterson (1983). The generation and control of roll motion of ships in closed turns. In: *Proc. 4th-IFAC/IFIP Symposium on Ship Operation Automation, Genova, Italy.*

Lewis, E.V., Ed.) (1988*a*). *Principles of Naval Architecture vol I: Stability and Strength.* third ed.. Society of Naval Architecture and Marine Engineers, New York.

Lewis, E.V., Ed.) (1988*b*). *Principles of Naval Architecture vol II: Resistance, Propulsion and Vibration.* third ed.. Society of Naval Architecture and Marine Engineers, New York.

Lewis, E.V., Ed.) (1988*c*). *Principles of Naval Architecture vol III: Motions in Waves and Controllability.* third ed.. Society of Naval Architecture and Marine Engineers, New York.

Price, W. C. and R. E. D. Bishop (1974). *Probabilistic theory of ship dynamics.* Chapman and Hall, London.

SNAME (1950). Nomenclature for treating the motion of a submerged body through a fluid. Technical Report Bulletin 1-5. Society of Naval Architects and Marine Engineers, New York, USA.

Son, K.H. and K. Nomoto (1982). On the coupled motion of steering and rolling of a high-speed container ship. *Naval Architecture and Ocean Engineering.*

van Amerongen, J. (1982). Adaptive steering of ships - A model reference approach to improved maneouvering and economic course keeping.. PhD thesis. Delft University of Technology, The Netherlands.

van Berlekom, W. B. (1975). Effects of propeller loading on rudder efficiency. In: *Proceedings 4th Ship Control Systems Symposium, Haag.* pp. 5.83–5.98.

van der Klugt, P.G.M. (1987). Rudder roll stabilization. PhD thesis. Delft University of Technology, The Netherlands.

Appendix A: Prime non-dimensional normalization system and conversion factors

The prime non-dimensionalization system of SNAME (1950) is the most commonly used by maritime institutions. In this system, the ship's length $L = L_{pp}$ is used as a linear measure unit, and the time unit U/L is the time requited to traveling a distance equal to the ship's length. U is the ship's total speed

$$U \triangleq \sqrt{u^2 + v^2}, \tag{60}$$

and ρ is the sea water density. Then, magnitudes are made non-dimensional as shown in Table 1[2].

Magnitudes	**Conversion**
Time	$t' = \frac{L}{U} \quad t$
Length and position	$\ell' = \frac{1}{L} \quad \ell \qquad x' = \frac{1}{L} \quad x$
Mass and Inertia	$m' = \frac{2}{\rho L^3} \quad m \qquad I' = \frac{2}{\rho L^5} \quad I$
Area	$a' = \frac{1}{L^2} \quad a$
Angle	$\alpha' = \alpha$
Forces	$F' = \frac{1}{\frac{1}{2}\rho U^2 L^2} F$
Moments	$M' = \frac{1}{\frac{1}{2}\rho U^2 L^3} M$
Linear velocity and acceleration	$v' = \dfrac{1}{U} \quad v \qquad \dot{v}' = \dfrac{L}{U^2} \quad \dot{v}$
Angular velocity and acceleration	$r' = \dfrac{L}{U} \quad r \qquad \dot{r}' = \dfrac{L^2}{U^2} \quad \dot{r}$

Table 3: Conversion to the Prime normalization system.

Some conversion factors between unit systems frequently used in marine applications:

Magnitude and units	**Conversion factor**
Angle	$\alpha_{rad} = \frac{\pi}{180} \quad \alpha_{deg}$
Linear speed: m/s and knots	$u_{kt} = \frac{3600}{1852} \quad v_{m/s}$
Angular speed: RPM and rad/s	$\omega_{rad/s} = \frac{2\pi}{60} \quad \omega_{RPM}$

Table 4: Conversion factors between unit systems.

[2]In table 1, $\rho = 1014 \quad (Kg/m^3)$ is the density of the sea water.

Appendix B: Main Data and RPMM model data for the Container ship

Main particulars

Quantity	Symbol	Measure	Unit
Length between perpendiculars	L_{pp}	230.66	m
Beam	B	32	m
Draft fore	D_f	10.7	m
Draft aft	D_a	10.7	m
Displacement	∇	46070	m^3
Nominal speed	U_{nom}	12.7	m/s
Block coefficient		0.561	
Transverse area of superstructure (sway)	A_Y	5200	m^2
Transverse area of superstructure (surge)	A_X	1100	m^2
Transverse Metacenter above keel	KM	15.18	m
Transverse Center of Buoyancy	KB	6.18	m
Transverse Metacenter	BM	$KM - KB$	m
Prismatic coefficient		0.595	
Nominal x coordinate of CG	x_G	-0.46	m
Nominal z coordinate of CG	z_G	-3.54	m
Nominal metacentric height	GM	0.83	m
Nondim mass	m'	750.81 10^{-5}	
Nondim inertia in roll	I'_{xx}	1.30 10^{-5}	
Nondim. inertia in yaw	I'_{zz}	43.25 10^{-5}	
Rudder area	A_R	42	m^2
Rudder angle	δ_{max}	35	deg
Rudder stall	δ_{stall}	17	deg
Rudder speed, 1 pump	$\dot{\delta}_{\max}$	2.3	deg/s
Rudder speed, 2 pumps	$\dot{\delta}_{\max}$	4.6	deg/s

Table 5: Main data for container ship from late 1970's - even keel condition.

Non-dimensional RPMM model data for the Container ship

X-Coefficients * 10^{-5}	Y-Coefficients* 10^{-5}	N-Coefficients* 10^{-5}	K-Coefficients* 10^{-5}
$X_v = -24.0$	$Y_v = -725.0$	$N_v = -300$	$K_v = 25.0$
$X_{vv} = -1.0$	$Y_{vv} = 98.6$	$N_{vv} = 0.6$	$K_{vv} = 0.0$
	$Y_{v\|v\|} = -5801.5$	$N_{v\|v\|} = -712.9$	$K_{v\|v\|} = 99.2$
$X_\delta = -1.4$	$Y_\delta = 248.1$	$N_\delta = -128.9$	$K_\delta = -6.5$
$X_{\delta\delta} = -116.8$	$Y_{\delta\delta} = 13.4$	$N_{\delta\delta} = -11.9$	$K_{\delta\delta} = -0.8$
$X_u = -226.2$	$Y_{\delta\delta\delta} = -193.0$	$N_{\delta\delta\delta} = 101.4$	$K_{\delta\delta\delta} = 4.1$
$X_{uu} = -64.5$	$Y_{\delta u} = -379.4$	$N_{\delta u} = 196.9$	$K_{\delta u} = 8.9$
$X_{uuu} = -137.2$	$Y_{\delta\delta u} = -55.6$	$N_{\delta\delta u} = 12.8$	$K_{\delta\delta u} = 1.3$
	$Y_{\delta\delta\delta u} = 232.3$	$N_{\delta\delta\delta u} = -125.4$	$K_{\delta\delta\delta u} = -4.8$
$X_0 = 0.0$	$Y_0 = 4.7$	$N_0 = -0.6$	$K_0 = -0.1$
$X_{v\delta} = 124.5$	$Y_{0u} = -5.3$	$N_{0u} = 6.5$	$K_{0u} = 1.1$
$X_{v\delta\delta} = -341.0$	$Y_{\delta v} = -100.0$	$N_{\delta v} = -24.6$	$K_{\delta v} = 5.4$
$X_{vv\delta} = 0.0$	$Y_{\delta vv} = 189.2$	$N_{\delta vv} = -349.1$	$K_{\delta vv} = -0.9$
$X_{\delta u} = -17.2$	$Y_{\delta\|v\|} = 0.0$	$N_{\delta\|v\|} = 0.0$	$K_{\delta\|v\|} = 0.0$
$X_{\delta\delta u} = 224.9$			
$X_\phi = -5.9$	$Y_\phi = 37.7$	$N_\phi = -17.9$	
$X_{\phi\phi} = -42.2$	$Y_{\phi\phi} = 0.0$	$N_{\phi\phi} = 0.0$	
$X_{v\phi} = 108.1$	$Y_{v\phi} = 144.9$	$N_{v\phi} = 17.8$	$K_{v\phi} = -14.7$
$X_{v\phi\phi} = 0.0$	$Y_{v\phi\phi} = 2459.3$	$N_{v\phi\phi} = -0.9$	$K_{v\phi\phi} = -103.9$
$X_{\phi vv} = 0.0$	$Y_{\phi vv} = 177.2$	$N_{\phi vv} = -933.9$	$K_{\phi vv} = -6.2$
$X_r = 43.1$	$Y_r = 118.2$	$N_r = -290.0$	$K_r = 0.8$
$X_{rr} = 4.4$	$Y_{r\|r\|} = 0.0$	$N_{r\|r\|} = 0.0$	$K_{r\|r\|} = -20.0$
	$Y_{rrr} = -158.0$	$N_{rrr} = -224.5$	$K_{rrr} = 0.0$
$X_{vr} = -24.0$	$Y_{r\|v\|} = -409.4$	$N_{r\|v\|} = -778.8$	$K_{r\|v\|} = 41.1$
	$Y_{rvv} = -994.6$	$N_{rvv} = -1287.2$	$K_{rvv} = -34.6$
	$Y_{v\|r\|} = -1192.7$	$N_{v\|r\|} = -174.7$	$K_{v\|r\|} = 10.4$
	$Y_{vrr} = -1107.9$	$N_{vrr} = 36.8$	$K_{vrr} = 22.2$
$X_{\dot{u}} = -124.4$	$Y_{\dot{r}} = -48.1$	$N_{\dot{r}} = -30.0$	$K_{\dot{r}} = -1.0$
	$Y_{\dot{v}} = -878.0$	$N_{\dot{v}} = 42.3$	$K_{\dot{v}} = 0$
	$Y_p = -3.4$	$N_p = -8.0$	$K_p = -3.0$
$X_{pp} = 7.2$	$Y_{p\|p\|} = 0.0$	$N_{p\|p\|} = 0.0$	$K_{p\|p\|} = -1.0$
	$Y_{ppp} = -9.3$	$N_{ppp} = 0.0$	$K_{ppp} = 0.0$
$X_{ppu} = 3.9$	$Y_{pu} = 23.6$	$N_{pu} = 12.8$	$K_{pu} = 0.0$
	$Y_{pu\|pu\|} = -52.5$	$N_{pu\|pu\|} = 0.0$	$K_{pu\|pu\|} = 0.0$
	$Y_{\dot{p}} = 23.3$	$N_{\dot{p}} = 0.2$	$K_{\dot{p}} = -0.7$

Table 6: Non-dimensional RPMM model test data for container ship.

Appendix C: Main Data and RPMM model data for a Multipurpose Naval Vessel.

Main particulars

Published with permission of the Danish Naval Material Command and Danish Maritime Institute.

Quantity	**Symbol**	**Measure**	**Unit**
Length between perpendiculars	L_{pp}	48	m
Beam	B	8.6	m
Draft	D	2.2	m
Displacement	∇	350	m^3
Nominal speed	U_{nom}	8	m/s
Nominal x coordinate of CG	x_G	-3.38	m
Nominal z coordinate of CG	z_G	-1.75	m
Nominal metacentric height	GM	0.776	m
Nominal mass	$m = \nabla\rho$	35.6 10^4	Kg
Nominal inertia in roll	I_{xx}	3.4 10^6	Kgm^2
Nominal inertia in yaw	I_{zz}	60 10^6	Kgm^2
Trans. Metacenter above keel	KM	4.72	m
Trans. Center of Buoyancy	KB	1.80	m
Trans. Metacenter	BM	$KM - KB = 0.97$	m
Rudder area	A_R	2×1.3	m^2
Max. rudder angle	δ_{max}	45	deg
Max. rudder speed	$\dot{\delta}_{max}$	20	deg/s
Stall angle	δ_{stall}	25	deg
Proportional band	δ_{pb}	4	deg
Dist. to CP	l_x	-23.5	m
Dist. to CP port	l_{yp}	-3.2	m
Dist. to CP starboard	l_{ys}	3.2	m
Dist. to CP	l_z	1.5	m
Tilt ang. port	θ_{tilt}	6	deg
Tilt ang. starboard	θ_{tilt}	-6	deg
Lift coefficient	C_L	1.15	

Table 7: Main data for a Multipurpose Naval Vessel at project stage.

X-Coefficients	N-Coefficients	K-Coefficients	Y-Coefficients
$X_{\dot{u}} = -17400$	$N_{\dot{v}}$=538000	$K_{\dot{u}}$=296000	$Y_{\dot{u}} = -393000$
$X_{u\|u\|} = -1960$	$N_{\dot{r}} = -38.7 \times 10^6$	$K_{\dot{r}}$= 0.0	$Y_{\dot{r}} = -1.4 \times 10^6$
X_{vr}= $0.33 \times m$	$N_{\dot{p}}$=0.0	$K_{\dot{p}} = -0.774 \times 10^6$	$Y_{\dot{p}} = -0.296 \times 10^6$
	$N_{\|u\|v} = -92000$	$K_{\|u\|v} = 9260$	$Y_{\|u\|v} = -11800$
	$N_{\|u\|r} = -4.71 \times 10^6$	$K_{ur} = -102000$	$Y_{ur} = 131000$
	$N_{v\|v\|} = 0.0$	$K_{v\|v\|} = 29300$	$Y_{v\|v\|} = -3700$
	$N_{r\|r\|} = -202 \times 10^6$	$K_{r\|r\|} = 0.0$	$Y_{r\|r\|} = 0.0$
	$N_{v\|r\|} = 0.0$	$K_{v\|r\|} = 0.621 \times 10^6$	$Y_{v\|r\|} = -0.794 \times 10^6$
	$N_{r\|v\|} = -15.6 \times 10^6$	$K_{r\|v\|} = 0.142 \times 10^6$	$Y_{r\|v\|} = -0.182 \times 10^6$
	$N_{\phi\|uv\|} = -0.214 \times 10^6$	$K_{\phi\|uv\|} = -8400$	$Y_{\phi\|uv\|} = 10800$
	$N_{\phi u\|r\|} = -4.98 \times 10^6$	$K_{\phi\|ur\|} = -0.196 \times 10^6$	$Y_{\phi\|ur\|} = 0.251 \times 10^6$
	$N_{\phi u\|u\|} = -8000$	$K_{\phi uu} = -1180$	$Y_{\phi uu} = -74$
	$N_{\|u\|p} = 0.0$	$K_{\|u\|p} = -15500$	$Y_{\|u\|p} = 0.0$
	$N_{p\|p\|} = 0.0$	$K_{p\|p\|} = -0.416 \times 10^6$	$Y_{p\|p\|} = 0.0$
	$N_p = 0.0$	$K_p = -0.5 \times 10^6$	$Y_p = 0.0$
	$N_\phi = 0.0$	$K_{\phi\phi\phi} = -0.325\rho g\nabla$	$Y_\phi = 0.0$
	$N_{\phi\phi\phi} = 0.0$		$Y_{\phi\phi\phi} = 0.0$
			$Y_{\delta uu} = 2 \times 3.5044 \times 10^3$

Table 8: Dimensional RPMM model test data for a Multipurpose Naval Vessel[3].

[3]Sea water density $\rho = 1014(Kg/m^3)$, Gravity constant $g = 9.80665 \quad (m/s^2)$.